⊙ 研究論文

Fullly Developed Turbulent Flow and Heat Transfer in Concentric Annuli with Square - Ribbed Roughness

S. W. Ahn* · S. K. Oh*

사각형 거칠기가 있는 동심이중관 내의 완전히 발달된 난류유동과 열전달

안 수 환 · 오 세 경

Key words : Turbulent flow(난류유동), Roughness pitch(조도 피치), Friction factor ratio(마찰계수비), Heat transfer ratio(열전달비).

Abstract

동심 이중관내에서 외관내벽의 사각돌출형 조도요소에 의한 비대칭 난류유동과 열전달 특성을, 열전달과 마찰계수에 미치는 조도의 합성효과를 조사하기위해, 연구하였다. 이론해석에서는 수정 플란틀 혼합길이(mixing length)이론의 난류모델을 속도분포와 마찰계수를 구하는데 사용하였다. 최대속도지점에서 안쪽과 바깥쪽의 두 속도형상들은 힘의 평형에 의해 일치 시켰다. 그리고나서, 온도 분포와 열전달 계수를 계산하였다. 속도형상과 마찰계수들의 해석 결과는 반경비 (α)=0.13, 0.26, 0.4, 그리고 0.56 경우의 실험과 매우 잘 일치하였다. 마찰계수와 Nusselt number에 미치는 반경비, 조도비, 그리고 조도에 대한 피치비등과 같은 여러 변수들의 효과들을 조사하였다. 본 연구는 일정 조도 요소들이 전체적 효율 측면에서 볼때 열전달을 유리하게 향상시킨다는 것을 증명하였다.

Nomenclature(see also Fig. 1)

a	thermal diffusivity	r	distance in radial direction
C	constant	R_j^+	$R_j(\tau_{Ro}/\rho)^{0.5}/\nu$
De	equivalent diameter	S	$R_o - R_i$
K	mixing length constant	T_j^+	$(T_{Ri} - T_j)C\tau_{Ro}/[q_{Ro}(\tau/\rho)^{0.5}]$
P	pitch, between tips of roughness elements	u_j^+	$u_j/(\tau_{Ro}/\rho)^{0.5}$
Pr_t	turbulent Prandtl number	y_j^+	$y_j(\tau/\rho)^{0.5}/\nu$
q	heat flux	Z_{ro}	imaginary location where $u_i=0$
		α	radius ratio, R_i/R_o
		δ_j	$\lvert R_m - R_j \rvert$

* 통영수산전문대학 기관과

Δ δ_j^+/R_j^+

ε eddy diffusivity

ε roughness height

ζ_j y_j^+/δ_j^+

Subscripts :

H Heat

i inner

j i or o

M momentum

m corresponding to the location of maximum velocity

o outer

R radius

r rough

s at sublayer boundary ; smooth

t turbulent

1. Introduction

The flow in annular ducts has received considerable attention and it appears often in many areas of the thermal process industries and in fluid flow equipment. An annular geometry has long been recognized as an important flow channel employed for the design of heat exchangers and fuel burners. In nuclear engineering, it has served as a basic geometry in evaluating the heat transfer performance of various type of reactor elements including, not only single ribbed pins in asmooth cylinders, but also more complex geometries such as rod bundles in circular or non – circular channels. Annulus flow is an axisymmetric geometry which, in the limiting cases, is reduced to the circular pipe and plane channel. For this reason, it has attracted the attention of researchers in the hope that its analysis would elucidate some of the evident difference between these two basic flow situations. However, they have investigated the turbulent flow and heat transfer in smooth annuli ; while there are quite a few literatures[1,2,3,4] on the turbulent flow and heat transfer in rough annuli. In heat exchangers with enhanced heat transfer surfaces which are sufficiently rough can increase heat transfer coefficients because the turbulence setup in the wake of each roughness element penetrate into the laminar sublayer. Therefore, it is generally expected that the effect would be greater for fluid with a higher Prandtl number. For the completely rough region in duct follow with relatively coarse and tightly spaced roughness elements, the friction factor is shown to be independent of the Reynolds number. Since the roughness of the surface not only increases the heat transfer rate, but also causes additional pressure losses, the heat transfer per unit pumping power expended may not be improved. Therefore, it is desirable to obtain optimum or advantageous geometrical shapes and arragements of the surface roughness elements. Schlichting[5] introduced the concept of equivalent sand grain roughness, K_s, as means of characterizing different types of surface roughness by referring to the equivalent net effect produced by Nikuradse's experiments, which were carried out in pipes that were artificially roughened with uniform grains of sand. Some other attempts[6] have been made to set up models of turbulent flow over the rough surfaces. Unfortunately, all these models require a prior knowledge of the function to describe a particular set of shapes and arragements of surface roughness elements. For such cases, there seems to be no reliable prediction for momentum and heat transfer available in the literature.

In our previous report[7], a different approach from these models was used to indirectly describe a particular surface roughness for the prediction of pressure loss and heat transfer

rate in an asymmetric flow induced by the given roughness elements, in which we obtained the turbulent flow and heat transfer in annuli with the square - ribbed roughness only on the outer tube using a turbulent flow model from Z_{ro}. In present study, it is assumed that the surface roughness affects only locally the velocity profiles, and therefore an empirical roughness correlation obtained for the flow in annuli with square - ribbed surface roughness elements on the outer tube only could be used in the analysis. The resultant effect of artificial roughness is determined from a comparison of rough and smooth annuli's results[8] using the heat transfer increase relative to the increase in pressure losses. Accordingly, the desirable artificial roughness structure in annuli has been obtained.

2. Analytical Study

The governing equations are broken into two in the smooth and rough sides. For the analysis, we introduce the following assumptions(see Fig. 1) :

(i) The annuli is concentric. While the outer wall surface is square - ribbed and insulated, the inner core surface is smooth and heated as constant heat flux.

(ii) Velocity and temperature fields in the annulus are fully developed.

(iii) The line of the maximum velocity coincides with the line of the zero shear stress.

(iv) For the smooth wall region, by van Driest's turbulent model[9] for the sublayer, and that of Reichardt[10] for the fully turbulent region are used.

(v) For the rough wall region, a modified logarithmic velocity profile is used.
The surface roughness affects only locally on the velocity profiles.

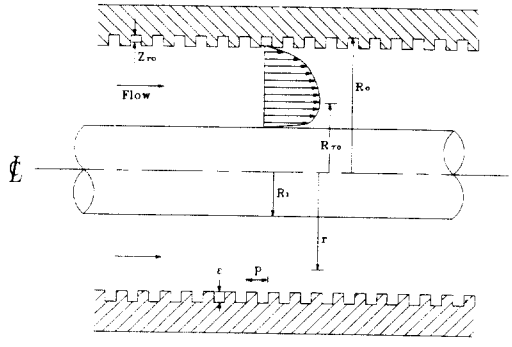

Fig. 1 Idealized Model

(vi) The turbulent Prandtl number is taken as unity.

For the velocity and temperature distributions, use is made of the concept of eddy diffusivity, ε, and the turbulent Prandtl number, Pr_t . The basic equations governing the transport of momentum and heat can thus be written as :

$$\frac{\tau}{\rho} = (\nu + \varepsilon_M)\frac{\partial u}{\partial y} \tag{1}$$

$$-\frac{q}{c\rho} = (a + \varepsilon_H)\frac{\partial T}{\partial r} \tag{2}$$

(1) can be non - dimensionalized as :

$$\frac{\partial u_i^+}{\partial \zeta_i} = \delta_i^+ \frac{\left(\frac{\tau}{\tau_R}\right)_i}{1+(\varepsilon_M/\nu)} \quad (0 \le \zeta_i \le 1) \tag{3}$$

$$\frac{\partial u_o^+}{\partial \zeta_o} = \frac{1}{u_{\tau_o}}\left(\frac{1}{K_i\zeta_i}\right) \quad \left(\frac{Z_{ro}^+}{\delta_o^+} \le \zeta_o \le 1\right) \tag{4}$$

where from a force balance. the shear stress distribution is :

$$\frac{\tau_i}{\tau_{Ro}} = \frac{[\alpha_{mo}^2 - \alpha^2(1+\Delta_i\zeta_i)^2]\left(1-\frac{Z_{ro}^+}{\delta_o^+}\Delta_o\right)}{(1+\Delta_i\zeta_i)\left[\left(1-\frac{Z_{ro}^+}{\delta_o^+}\right)^2 - \alpha_{mo}^2\right]\alpha} \tag{5}$$

$$\frac{\tau_o}{\tau_{Ro}} = \frac{\left(1-\frac{Z_{ro}^+}{\delta_o^+}\Delta_o\right)[(1-\Delta_o\zeta_o)^2 - \alpha_{mo}^2]}{(1-\Delta_o\zeta_o)\left[\left(1-\frac{Z_{ro}^+}{\delta_o^+}\right)^2 - \alpha_{mo}^2\right]} \tag{6}$$

The initial conditions for (3) and (4) are : $u_i^+ = 0$ at $\zeta_i = (Z_{Ro}^+/\delta_i^+)$ and $u_o^+ = 0$ at $\zeta_o = 0$. From (1) and (2), the following expressions[7] Can be also abtained as :

$$\frac{\partial T^+}{\partial \zeta} = \frac{\partial u^+}{\partial \zeta} \frac{(1+\varepsilon_M/\nu)}{(1/\mathrm{Pr}+1/P_{r_t}\varepsilon_M/\nu)} \frac{q_i/q_{Ri}}{(\tau_j/\tau_{Rj})} \quad (7)$$

where the heat flux distributions from an energy balance are :

$$\frac{q_i}{q_{Ri}} = \frac{1}{(1+\Delta_i\zeta_i)} \frac{\left[\left(1-\Delta_o\frac{Z_{ro}^+}{\delta_o^+}\right)^2 - \alpha^2(1+\Delta_i\zeta_i)^2\right]}{\left[\left(1-\Delta_o\frac{Z_{ro}^+}{\delta_o^+}\right)^2 - \alpha^2\right]} \quad (8)$$

$$\frac{q_o}{q_{Ri}} = \frac{\alpha}{(1+\Delta_o\zeta_o)} \frac{\left[\left(1-\Delta_o\frac{Z_{ro}^+}{\delta_o^+}\right)^2 - (1-\Delta_o\zeta_o)^2\right]}{\left[\left(1-\Delta_o\frac{Z_{ro}^+}{\delta_o^+}\right)^2 - \alpha^2\right]} \quad (9)$$

The initial conditions for (7) are :

$T_i^+ = 0$ at $\zeta_i = 0$.

The dimensionless velocity and temperature distributions in the inner and outer regions of the maximum velocity(see Fig. 1) can be obtained by solving these differential equations, (3), (4) and (7), once the eddy diffusivities and the matching conditions are established. Accuracy of description of the eddy diffusivity for momentum along and across the duct is required for the solution of velocity and temperature profiles. The most interesting feature of the study on the turbulent fluid flow in a concentric annular duct is the complete failure in application of the conventional universal velocity profile or the law of wall[8]. Since the assumption of an eddy diffusivity of zero at the pipe line is not realistic, we postulate that Reichardt's expression[10] for the eddy diffusivity of momentum can be applicable to the entire turbulent flow regions on the inner smooth wall region of the concentric annulus with proper modification for the region remote from the inner wall. Thus, using the dimensionless parameters, we can obtain the equation as follows :

for sublayer, $(0 \le y_i^+ \le y_{is}^+)$:

$$\left(\frac{\varepsilon_M}{\nu}\right)_i = K_i^2 y_i^{+2}[1-\mathrm{EXP}(-y_i^+/A_i^+)]^2\left|\partial u_i^+/\partial y_i^+\right| \quad (10)$$

for fully developed turbulent flow,
$(y_{is} \le y_i^+ \le \zeta_i^+)$:

$$(\varepsilon_M/\nu)_t = \frac{u_{\tau Ro}}{u_{\tau Ro}}\frac{K_i}{6}\delta_i^+[1-(1-\zeta_i)^2][1+2(1-\zeta_i)^2] \quad (11)$$

and for the rough region, $(Z_{ro}^+ \le y_o^+ \le \delta_o^+)$:

$$(\varepsilon_M/\nu) = \frac{K_o^2 y_o^{+2}}{\nu}\left|\frac{\partial u_o^+}{\partial y_o^+}\right| \quad (12)$$

where

$$u_o^+ = \frac{1}{K_o}\ln\left(\frac{y_o^+}{Z_{ro}^+}\right) \quad (13)$$

and

$$Z_{ro}^+ = y_{mr}^+ \mathrm{EXP}\left[-\frac{u_{\tau_i}}{u_{\tau_o}}[\ln[R_o^+(1-\alpha)-y_{mr}^+]\times \frac{u_{\tau_i}}{u_{\tau_o}} + C\,K_i\right] \quad (14)$$

from the experimental study :

$$y_{mr} = 0.299S(2.167-2.65X10^{-6}\mathrm{Re})\left(\frac{S}{\varepsilon}\right)^{0.140}\left(\frac{P}{S}\right)^{0.201}(3.74-24.87\alpha+77.9\alpha^2-73.9\alpha^2) \quad (15)$$

Now that the eddy diffusivities (ε_M/ν) are known for the entire fluid region, the velocity and temperature profiles can be derived. The Reynolds number, friction factor, heat transfer

coefficient and Nusselt number can be obtained in the usual way. The Reynolds number is defined as :

$$\mathrm{Re} = u_b 2(R_o - R_i)/\nu = 2u_b^+(R_o^+ - R_i^+) \qquad (16)$$

The bulk velocity(u_b) can be expressed as :

$$u_b = \frac{\int_{R_i}^{R_m} u\, 2\pi r\, dr}{\pi(R_o^2 - R_i^2)} + \frac{\int u\, 2\pi r\, dr}{\pi(R_o^2 - R_i^2)} \qquad (17)$$

And dimensionless form of equation (17) becomes as follows :

$$u_b = \frac{\nu}{R_o}\frac{2}{1-\alpha^2}\left[\delta_o^+\int_{\frac{Z_{ro}^+}{\delta_o^+}}^{1}\frac{1}{K_o}\ln\left(\delta_o^+\frac{\zeta_o}{Z_{ro}^+}\right)(1-\Delta_o\zeta_o)d\zeta_o + \alpha\delta_i^+\int_0^1(1+\Delta_i\zeta_i)d\zeta_i\right] \qquad (18)$$

Friction factor in a dimensionless form from the usual definition yields :

$$f = 8\frac{(1-\alpha)^2}{(1+\alpha)}\frac{R_o^{+2}}{\mathrm{Re}^2}\left[1+\left(\frac{u_{\tau_i}}{u_{\tau_o}}\right)^2\right] \qquad (19)$$

From the definition, the Nusselt number is :

$$Nu = \frac{2h(R_o - R_i)}{k} = 2[1-\alpha]\frac{R_o^+\mathrm{Pr}}{T_b^+} \qquad (20)$$

where $h = q_{Ri}/(T_{Ri} - T_b)$

Bulk temperature(T_b) can be obtained in dimensionless form as follows :

$$T_b^+ = \frac{4}{\mathrm{Re}(1+\alpha)}\left[\int_0^{R_m^+ - R_i^+}\left(\alpha + \frac{y_i^+}{R_o^+}\right)u_i^+ T_i^+ dy_i^+ + \int_{R_m^+ - R_i^+}^{R_o^+ - R_i^+ - Z_{ro}^+}\left(\alpha + \frac{y_o^+}{R_o^+}\right)u_o^+ T_o^+ dy_i^+\right] \qquad (21)$$

Since there is within about 5% deviation between the maximum velocity and zero shear stress position in all the cases as in Fig. 2, it can be assumed that two positions are coincident ; therefore, shear stress ratio from a force balance using maximum velocity position becomes :

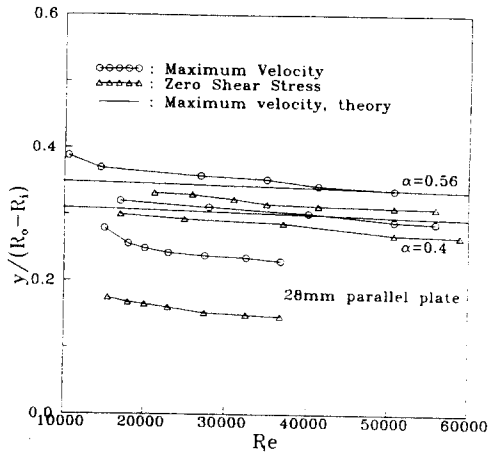

Fig. 2 Maximum velocity position versus zero shear stress position

$$\frac{\tau_{Ri}}{\tau_{Ro}} = \frac{R_o - Z_{Ro}}{R_i}\left[\frac{R_m^2 - R_i^2}{(R_o - Z_{ro})^2 - R_m^2}\right] \qquad (22)$$

It is well established that the standard universal velocity is not fully adequate for the inner velocity distribution of a concentric annulus. Therefore, a fixed value of 0.4 for K_o is taken. Using the values of K_i and C from the dimensionless velocity profile by experiment, the dimensionless velocity profiles in accordance with radius ratio(α) are obtained as $u^+ = (3.21 - 1.19\alpha - 4.544\alpha^2 + 6.16\alpha^3)\, y^+ + (6.68 - 6.6\alpha - 32.36\alpha^2 + 58.5\alpha^3)$. From the continuity of velocities at the location of the maximum velocity, ($r = R_m$, or $\zeta_i = \zeta_o = 1$), the maximum dimensionless velocity position becomes :

$$u_{om}^+ = u_{im}^+ \qquad (23)$$

From the equality of temperature at the location of maximum velocity(i.e. $r = R_m$ or $\zeta_i = \zeta_o = 1$), the matched dimensionless temperature position between the inner and outer wall regions is :

$$T_{om}^+ = T_{im}^+ \qquad (24)$$

and

$$\frac{\partial T_{im}^{+}}{\partial \zeta_i} = -\frac{\partial T_{om}^{+}}{\partial \zeta_o}\frac{\delta_i^{+}}{\delta_o^{+}} \tag{25}$$

In order to obtain the results for the given Reynolds number, first of all, a Reynolds number should be given ; however, the Reynolds number is actually obtained from the velocity profile, and the velocity profile is obtained from the given Reynolds number. Therefore, a two - dimensional iteration method is used : one is for the velocity, and the other is for the Reynolds number. For the initial guess, a dimensionless sublayer thickness(ζ_{sub}) is used. The dimensionless sublayer thickness(ζ_{sub}) is the number between 0 and 1, so that R_o^+ and R_m^+/R_o^+ are the variables of Reynolds number. With the guessed R_m^+/R_o^+, the velocity profiles in the smooth and rough parts are obtained by a numerical method where we use the 5 - point Gaussian quadrature integration method. At the maximum velocity position, we check the equality of velocity. With the condition that velocities of both parts are equal, the Reynolds number is calculated with the velocity profiles obtained from the Simpson's integration method with the number of nodes equal to 5000. If the velocities are not equal, we reguess the value of R_m^+/R_o^+. If the calculated Reynolds number is equal to the given Reynolds number, the velocity profile is obtained. Finally, the friction factor, temperature profile, bulk temperature, and Nusselt number are calculated. And we use the parameters in calculation as follows :

Table 1 Parameters used in calculation

	class	range
Input parameters	α	0.13,0.26, 0.4, and 0.56
	R_o^+	in terms of Re ; 10^4 to 10^5
	Pr	0.1, 0.72, 1.0, 7 and 30
	P/ε	2
	S/ε	14.3, 19.5, 24,and 28.2
	Pr_t	1
Fixed parameters	A_i^+	26(van Driest damping parameter)
	y_{is}^+	26(sublayer thickness)

3. Experimental Study

In the analytical study, the theoretical analyses that presented and predicted velocity profiles, friction factors, temperature profiles, and Nusselt numbers for the developed region of concentric annulus with a roughness on the outer tube were evaluated. The experimental programme undertaken in the present study is designed to meet some of the research objectives described before, i.e., velocity profiles, friction factors, maximum velocity and zero shear stress positions. The working fluid is chosen as air in atmospheric conditions due to purposes of economical construction of test facilities and also availability of information on physical properties. The static pressure measurements are made with a MKS pressure transducer and the calibration of which is checked against a micro - manometer at frequent intervals. Velocities are measured with a single pitot tube and x - type hot wire anemometer, and maximum velocity and zero shear stress positions are measured with a double pitot tube and a x - type hot wire anemometer at the radius ratios(α=0.13, 0.26, 0.4, and 0.56), respectively.

As is seen in Fig. 3, the total dimension of the main apparatus is about 6.1 meter in length. Air is drawn through a flow measuring orifice into an air filter and then through a bell - mouthed contraction section into the test section by a blower(0.8KW, 3400RPM) located at the extreme downstream end. The bell - mouthed section(miminum inner diameter, 97mm ; maximum inner diameter, 160mm) is

Table 2 Essential dimensions unit : mm

	O. D	I. D	material	α(Ri/Ro)	De
outer tube	117.6	97	Al - alloy		
core tube	12.4, 25.4, 38.4, and 54	10.8, 23.8, 36.7, and 52	copper	0.13, 0.26, 0.4, and 0.56	84.5, 71.8 58.4, and 43

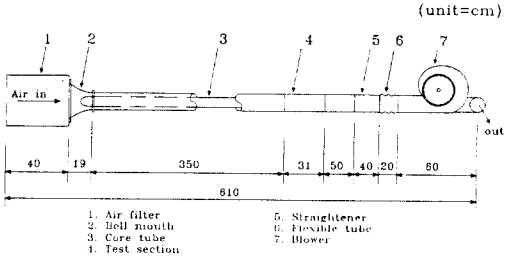

Fig. 3 Schematic diagram of experimental setup

1. Air filter
2. Bell mouth
3. Core tube
4. Test section
5. Straightener
6. Flexible tube
7. Blower

made of cast iron and the blower fan is rated 9 cubic m/min at 520mmAq.

Along the annular test section, which consists of 12.4, 25.4,38.4, and 54mm O.D. inner tubes with a 97mm I.D. outer tube with ε of 1.5 mm as in Table 2. A specially designed traversing mechanism carried the measuring instrument.

With this mechanism, the relative radial displacement of a probe was measured within 0. 025mm by electrical contact. The core tubes are supported at three locations by 3 - point carriers which allow for radial adjustments of the core tube. When the test sections were assembled and aligned, the concentricity of the core to the outer tube was checked. The eccentricity due to the lack of straightness of the tubes was negligible in most cases, but a maximum of 2% was noted. The orifice of the flow rate measurement was calibrated by numerical integration of the velocity profiles measured at test sections. Steady state conditions were maintained for at least one - half hour before measurement were made. Pressure drop data were obtained over the entire accessible Reynolds number range whose upper limit was restricted by the blower capacity. Velocity profiles were explored with a total tube together with the static pressure taps provided on the outer tube of the annulus. The range of Reynolds number covered is from 15,000 to 92, 000 approximately. The pressure and temperature of the ambient are also recorded before each run. All the measurements were carried out only late in the night to avoid disturbances on the main power supply.

The main experimental variables for the present study are the radius ratio (α), pitch of the roughness (P) and the ratio of distance between inner and outer tube to roughness height (S/ε), for roughness pitch ratio (P/ε=2). In x - type hot wire anemometer system the constant temperature type anemometer(C.T.A., TSI Model 1054 A) and general wave analyzer (D - 6000 Model 611, Data Precision Inc.) are used and calibration is done with the pitot tube of 4mm in diameter and 350mm in length and digital micro - manometer(Model FC012). The outputs from C.T.A. Bridge that are prevented from aliazing by passing through 5 KHz low - pass filter are simutaneously sampled as digital values by means of 14 - bit A/D converter and Sample and Holder contained in general wave analyzer, and then are recorded at the diskettes through Data Recorder, at which the sampling rate becomes 10,000units per second corresponding to Niquist sample period.

4. Results and Discussion

An example of predicted velocity profiles is compared with the experimental measurement in Fig. 4. In general the velocity profiles obtained through (3), (4) and by (18) agree reasonably well with the experimental data. The data for other ranges of parameters showed similar trend.

The developed region can be known from the measurement of static pressure drops versus channel length from entrance, x, and at developed region from x=1.28m, values of dp/dx are calculated as a function of x by fitting a straight line into the data points taken five at a time and taking the slope of this line as the dp/dx. The friction factor, f, is obtained by substituting dp/dx and Reynolds number into equation(19).

The effects of α on the friction factors obtained from the zero shear stress positions in Fig. 2 and the static pressure drops are shown in Fig. 5, at which the friction factor is largest at the case of $\alpha=0.4$, and is higher in annuli with the outer tube roughness rather than in those with core tube roughness. In Fig. 6, the increase in pressure loss in terms of friction factor due to the roughness elements on the outer tube is normalized by that of the smooth case verified by experiment[8].

The normalized friction factor is defined as ;

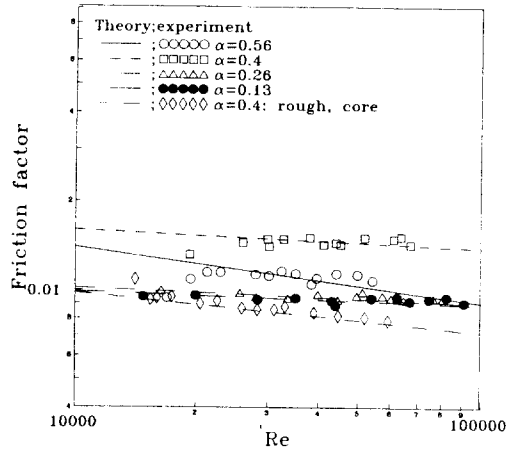

Fig. 5 Friction factor

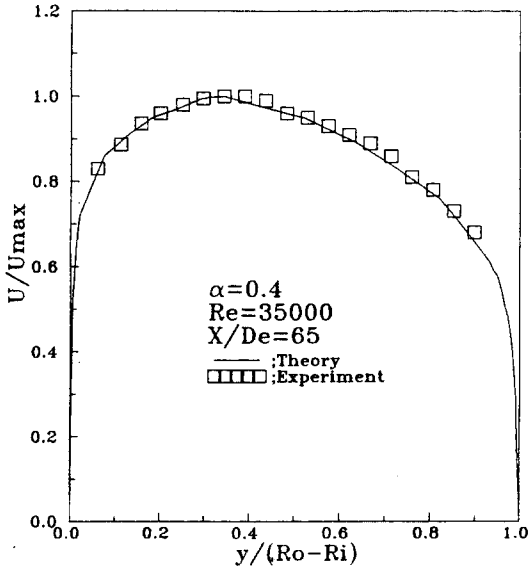

Fig. 4 Velocity distribution

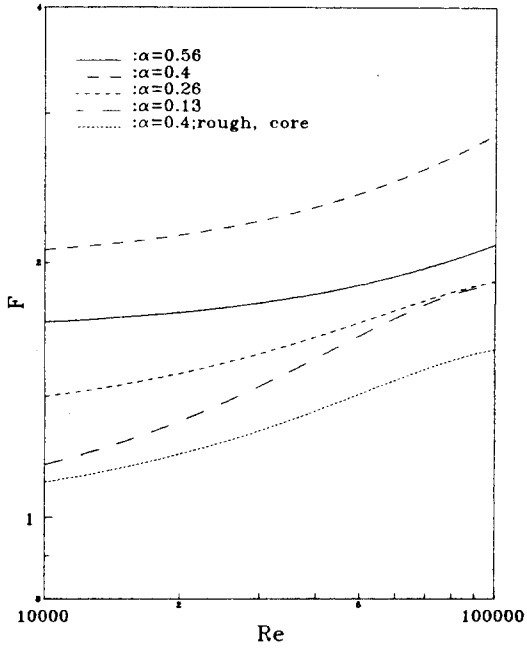

Fig. 6 Friction factor ratio, F

$$F=f_r/f_s \tag{26}$$

It can be seen that the effect of α is significant. F is highest at α=0.4 for the range of the parameters studied. This tendency is attributed from the fact that the friction factor is subjected to the change of the static pressure drop, velocity, and equivalent diameter.

Heat transfer in terms of Nu is also normalized as :

$$H=Nu_r/Nu_s \tag{27}$$

The effects of α and Pr on H is seen in Fig. 7 and the trends are similar to those observed in Fig. 6. The resultant effect of artificial roughness is determined from the comparison of rough and smooth surfaces with respect to the heat transfer increase relative to the increase in pressure losses. This is expressed in terms of a non - dimensional parameter, H/F, which is defined as :

$$H/F=(Nu_r/Nu_s)/(f_r/f_s) \tag{28}$$

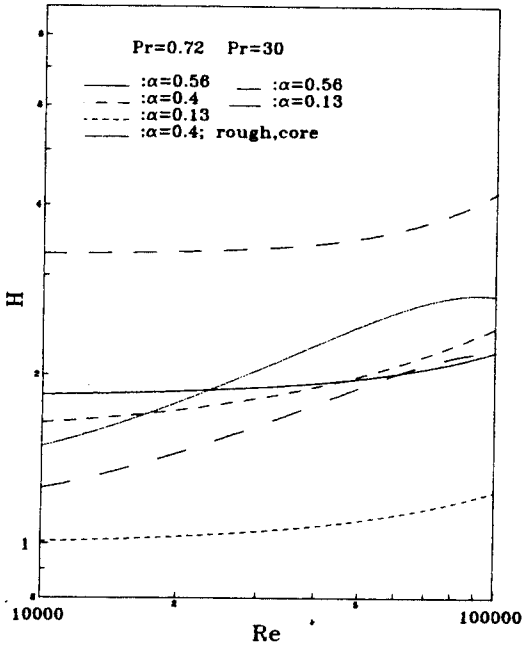

Fig. 7 Heat transfer ratio, H

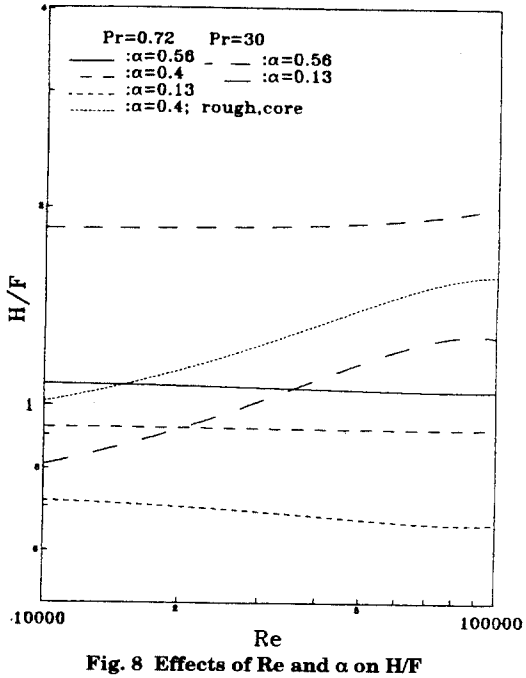

Fig. 8 Effects of Re and α on H/F

H/F>1 suggests that the increase in heat transfer due to roughness is greater than the increase in pressure loss due to roughness. Therefore, it is advantageous to have the particular roughness elements in the overall efficiency point of view.

Fig. 8 shows the effects of the Reynolds number and radius ratio(α). The ratio of H/F increases with increasing Pr and α at the case of Pr=0.72, and is higher in annuli with the rough core tube rather than with the rough outer tube because it is assumed in the analysis that the core tube is heated as constant heat flux, while the outer tube is insulated.

5. Conclusion Remarks

From the analytical and experimental investigation on the drag force and heat transfer characteristics in the developed region of turbulent fluid flow in concentric annulus with a uniformly heated smooth core tube and with

the square - ribbed outer tube, the conclusion can be derived that the effects of radius ratio (α), roughness density, relative roughness height, Reynolds and Prandtl numbers on the ratio H/F were identified for the turbulent flow induced by square - ribbed surface roughness elements on the outer tube of a concentric annulus. The study demonstrates that certain artificial roughness elements can be used to enhance heat transfer rates with advantages from the overall efficiency point of view. The required pumping power per unit heat transfer rate decreses with increasing value of α at the case of Pr=0.72 and increasing Prandtl numbers for the range of parameters studied.

Acknowledgement

This paper was supported in part by NON DIRECTED RESEARCH FUND, Korea Research Foundation,1992.

Reference

1) Durst, F., 1968, "On Turbulent Flow through Annular Passages with Smooth and Rough Core", M. Sc. Thesis, Imperial College.

2) 김 경천, 안 수환, 이 병규, 1993, "사각돌출형 거칠기가 있는 이중동심관 내의 난류측정", 대한기계학회 추계학술대회, 한양대학교 안산캠퍼스, 11월 6일. 제2권, pp. 85 - 89.

3) Lee, Y. P., Ahn, S. W. and Y. Lee, 1990, "Turbulent Fluid Flow and Heat Transfer Induced by Square - Ribbed Surface Roughness in Concentric Annuli", Ninth International Heat Transfer Conference, 4 - MC - 20, Jerusalem, August.

4) Lee, Y. P., Ahn, S. W. and Y. Lee, 1990, "Enhanced Turbulent Heat Transfer Induced by Square - Ribbed Wall Roughness in Concentric Annuli", Proceedings of The Second KSME - JSME Fluids Engineering Conference, Seoul, Vol.2 pp. 293 - 298.

5) Schlichting, H., 1968, "Boundary Layer Theory", 6th ed.,McGraw Hill Book Co. Inc,. pp. 578 - 589.

6) Allan, W.K. and Sharma, V., 1974, "An investigation of Low Turbulent Flows over Rough Surface", Jour. Mech. Eng. Sci.,Vol. 16, pp. 71 - 78.

7) 안 수환, 이 윤표, 김 경천, 1993, "사각돌출형 표면거칠기가 있는 이중동심원관 내의 난류유동과 열전달", 대한기계학회논문집, 제17권, 제5호, pp. 1294 - 1303.

8) Park, S. D., 1971, "Developing Turbulent Flow in Concentric Annuli : An Analytical and Experimental Study", Ph. D. Thesis, Dept. of Mech. Eng., University of Ottawa.

9) van Driest, E. R.,1956, "On Turbulent Flow Near a Wall", J. of Aero. Sci., Vol.23, pp. 485.

10) Reichardt, H., 1951, "Vollstandige Darstellung der turbulenten Geschwindigekeitsverterilung in glatten Leitungen", Z. amgew. Mathematic und Mechanik, Vol. 31, pp. 208 - 219.